

State-space modal representations for decomposition of multivariate non-stationary signals

Luis David Avendaño-Valencia* Luis Enrique Avendaño**
Edilson Delgado-Trejos*** David Cuesta-Frau****

* *Vibration and Sound Research Group, Syddansk Universitet, Campusvej 55, 5230 Odense M, Denmark (e-mail: ldav@sdu.dk)*

** *Escuela de Tecnología Eléctrica, Universidad Tecnológica de Pereira, Cr. 27 No. 10-02, Pereira, Colombia (e-mail: leavenda@utp.edu.co)*

*** *AMYSOD Lab, CM&P Research Group, Instituto Tecnológico Metropolitano ITM, CL 73 No. 76 A 354, 050034 Medellín Colombia (e-mail: edilsondelgado@itm.edu.co)*

**** *Escuela Politécnica Superior de Alcoy, Universitat Politècnica de València, Pl. Ferrándiz Carbonell, 03801 Alcoy, España (e-mail: dcuesta@disca.upv.es)*

Abstract: This work introduces a parametric modal decomposition method for multivariate non-stationary signals based on a block-diagonal time-dependent state space representation and Kalman filtering/smoothing. Each second-order block is constructed with the real and imaginary parts of each mode instantaneous eigenvalues, and thus represents a single non-stationary oscillatory component. The identification of the state/parameter trajectories and the hyperparameters, constituted by the mode mixing matrix, the state, parameter and noise covariances, and initial conditions, is accomplished with a tailored Expectation-Maximization algorithm. The methodology is evaluated in a numerical example, concerning a multivariate signal with three modal components, featuring mode crossings and vanishing amplitudes. Codes and examples are available on <https://github.com/ldavendanov/NS-modal-decomposition>.

Keywords: Multivariable system identification, Bayesian methods, Non-linear system identification.

1. INTRODUCTION

Modal decomposition can be defined as the problem of separating a signal into a finite set of orthogonal oscillatory components. In the non-stationary case, the oscillatory components comprise sinusoids with time-dependent amplitude and frequency –or *instantaneous amplitude* (IA) and *instantaneous frequency* (IF)–. There are several well-established modal decomposition methods that can be applied on single (univariate) non-stationary signals, including: proper orthogonal decomposition (Lu et al., 2019), empirical mode decomposition (Hao et al., 2017), ridge tracking on time-frequency/time-scale representations (Iatsenko et al., 2016), and *synchro squeezing/extracting transforms* (Li et al., 2020). Main limitations of these non-parametric methods relate to the maximum feasible resolution in time-frequency domain, and their sensitivity to noise and signal singularities –*v.gr.* IF discontinuities/crossings, or vanishing amplitudes– (Iatsenko et al., 2016; Stanković et al., 2020).

Kalman filter (KF) frequency trackers constitute a parametric alternative to the estimation of modal decompositions (Dardanelli et al., 2010). These are based on second order *state space* (SS) modal representations describing a single sinusoidal component and its quadrature, while a

third state, representing the IF, is also appended. Considering the non-linear relation from the IF to the modes, through a trigonometric function, non-linear KF approximations are necessary (Dardanelli et al., 2010; Cardona-Morales et al., 2014; Brumana and Piroddi, 2020). A unifying framework has been presented in (Avendaño et al., 2018), where second order blocks, comprised by the real and imaginary parts of the instantaneous eigenvalue of the modal component, are introduced. These coefficients comprise a parameter vector, which is jointly estimated with the state (modal) vector. Whilst the resulting SS representation is larger, it also yields a milder bilinear non-linearity, which can be dealt better by an Extended KF. The performance of these methods is bound to the correct selection of the state, parameter and noise covariances. This selection is commonly left to the user. Nonetheless, optimization schemes based on the marginal likelihood or prediction error of the KF (Avendaño et al., 2018), or adaptive tracking (Brumana and Piroddi, 2020) have been proposed. Yet, to limit the number of parameters to optimize, the covariances are customarily defined diagonal, limiting the potential estimation accuracy, particularly when IFs of different components are correlated.

In contrast to the case of univariate non-stationary signals, the modal decomposition of multivariate (vector)

non-stationary signals has received less attention. Considering that multivariate signals provide a collective view of the underlying system, there is a latent potential for improved isolation of modal components and noise robustness (Stanković et al., 2020). Still, although multivariate non-stationary parametric system identification methods can be used to extract non-stationary modal features (Spiridonakos and Fassois, 2009; Zhou et al., 2018), direct parametric modal-domain identification has not been addressed yet. Such modeling methods would boast the parsimony and improved accuracy of parametric modeling methods, with the added advantage of direct tracking of non-stationary modal properties. In this work, we generalize the formulation provided in our previous work (Avenidaño et al., 2018) and extend it to the case of multivariate non-stationary signals. This requires the introduction of a mode mixing matrix, which needs to be identified. The mixing matrix together with the state, parameter and noise covariances and initial values are set as hyperparameters of the SS modal representation, and are subsequently estimated with a tailored Expectation-Maximization (EM) algorithm. The proposed methodology is evaluated in a numerical example, concerning a multivariate signal with three modal components, featuring mode crossings and vanishing amplitudes. The methodological framework is presented in Section 2, while the numerical example is presented in Section 3. The methods, the numerical example and others are available on the GitHub repository <https://github.com/ldavendanov/NS-modal-decomposition>.

2. METHODOLOGICAL FRAMEWORK

2.1 Time-dependent state-space modal representation

Consider the multivariate signal $\mathbf{y}_t \in \mathbb{R}^n$, obtained by the superposition of M non-stationary modal components as:

$$\mathbf{y}_t = \sum_{m=1}^M \boldsymbol{\psi}_m x_{m,t} + \boldsymbol{\varepsilon}_t, \quad \boldsymbol{\varepsilon}_t \sim \text{NID}(\mathbf{0}, \boldsymbol{\Sigma}_\varepsilon) \quad (1a)$$

$$x_{m,t} = A_{m,t} \cdot e^{j\phi_{m,t}} \quad (1b)$$

where $x_{m,t}$ is the m -th non-stationary modal component (*mode*) with IA $A_{m,t}$, and *instantaneous phase* (IP) $\phi_{m,t}$, while the mixing vector $\boldsymbol{\psi}_m \in \mathbb{R}^n$ represents the proportion of each modal component in the signal, and $\boldsymbol{\varepsilon}_t \in \mathbb{R}^n$ is the measurement noise, assumed a zero-mean *Normally and Independently Distributed* (NID) process with covariance matrix $\boldsymbol{\Sigma}_\varepsilon$. Each mode can be associated with the IF $\omega_{m,t}$ defined as (Boashash, 1992):

$$\omega_{m,t} = \frac{\partial}{\partial t} \phi_{m,t} \approx \frac{1}{T_s} (\phi_{m,t} - \phi_{m,t-1}) \quad (2)$$

where T_s is the sampling period. To avoid underdeterminacy of the coefficients in the mixing vector and the IA's, the modes $x_{m,t}$ are assumed to be orthonormal, so that $\langle x_{m,t}, x_{n,t} \rangle = 1$ if $m = n$, and zero otherwise.

As demonstrated in (Avenidaño et al., 2018), a single response signal $y_{k,t}$, $k = 1, \dots, n$ can be represented as the response of a block-diagonal SS system with time-dependent coefficients. This representation is hereby extended to the multivariate signal $\mathbf{y}_{m,t}$, as follows:

$$\mathbf{z}_t = \mathbf{M}(\boldsymbol{\theta}_{t-1}) \cdot \mathbf{z}_{t-1} + \mathbf{u}_t, \quad \mathbf{u}_t \sim \text{NID}(\mathbf{0}_M, \boldsymbol{\Sigma}_u) \quad (3a)$$

$$\boldsymbol{\theta}_t = \boldsymbol{\theta}_{t-1} + \mathbf{v}_t, \quad \mathbf{v}_t \sim \text{NID}(\mathbf{0}_M, \boldsymbol{\Sigma}_v) \quad (3b)$$

$$\mathbf{y}_t = \boldsymbol{\Psi} \cdot \mathbf{z}_t + \boldsymbol{\varepsilon}_t, \quad \boldsymbol{\varepsilon}_t \sim \text{NID}(\mathbf{0}_n, \boldsymbol{\Sigma}_\varepsilon) \quad (3c)$$

where the state vector $\mathbf{z}_t \in \mathbb{R}^{2M}$ and the parameter vector $\boldsymbol{\theta}_t \in \mathbb{R}^{2M}$ are both defined as:

$$\mathbf{z}_t := \begin{bmatrix} \Re\{x_{1,t}\} \\ \Im\{x_{1,t}\} \\ \vdots \\ \Re\{x_{M,t}\} \\ \Im\{x_{M,t}\} \end{bmatrix} \quad \boldsymbol{\theta}_t := \begin{bmatrix} \alpha_{1,t} \\ \beta_{1,t} \\ \vdots \\ \alpha_{M,t} \\ \beta_{M,t} \end{bmatrix} \quad (4)$$

with $\Re\{C\}$ and $\Im\{C\}$ indicating the real and imaginary parts of the complex number C . The measurement matrix $\boldsymbol{\Psi}$ and the state transition matrix $\mathbf{M}(\boldsymbol{\theta}_t)$ are defined as:

$$\boldsymbol{\Psi} = [\Re\{\boldsymbol{\psi}_1\} \Im\{\boldsymbol{\psi}_1\} \cdots \Re\{\boldsymbol{\psi}_M\} \Im\{\boldsymbol{\psi}_M\}] \quad (5a)$$

$$\mathbf{M}(\boldsymbol{\theta}_t) = \begin{bmatrix} \mathbf{M}_1(\boldsymbol{\theta}_t) & & \\ & \ddots & \\ & & \mathbf{M}_M(\boldsymbol{\theta}_t) \end{bmatrix} \quad (5b)$$

$$\mathbf{M}_m(\boldsymbol{\theta}_t) = \begin{bmatrix} \alpha_{m,t} & \beta_{m,t} \\ -\beta_{m,t} & \alpha_{m,t} \end{bmatrix}, \quad m = 1, \dots, M \quad (5c)$$

where $\alpha_{m,t} + j\beta_{m,t} = \lambda_{m,t}$ represents the instantaneous eigenvalue associated with the m -th mode, so that:

$$x_{m,t} = \prod_{\tau=1}^t \lambda_{m,\tau} = \prod_{\tau=1}^t \alpha_{m,\tau} + j\beta_{m,\tau} \quad (6)$$

$$A_{m,t} = \left| \prod_{\tau=1}^t \lambda_{m,\tau} \right|, \quad \phi_{m,t} = \arg \left(\prod_{\tau=1}^t \lambda_{m,\tau} \right) \quad (7)$$

The state innovations $\mathbf{u}_t \in \mathbb{R}^{2M}$, the parameter innovations $\mathbf{v}_t \in \mathbb{R}^{2M}$, and the measurement noise $\boldsymbol{\varepsilon}_t$ are zero-mean NID and mutually uncorrelated random processes, with respective covariances $\boldsymbol{\Sigma}_u \in \mathbb{R}^{2M \times 2M}$, $\boldsymbol{\Sigma}_v \in \mathbb{R}^{2M \times 2M}$ and $\boldsymbol{\Sigma}_\varepsilon \in \mathbb{R}^{n \times n}$. Due to the orthonormality condition of the modes, the state innovations covariance must be diagonal, so that $\boldsymbol{\Sigma}_u = \text{diag}(\sigma_{u_1}^2, \sigma_{u_2}^2, \dots, \sigma_{u_{2M}}^2)$ with $\sigma_{u_{2i}}^2 = \sigma_{u_{2i-1}}^2$, for all $i = 1, \dots, M$.

Equation (3a) defines a bilinear relation between the previous values of the state vector (representing the modes) and the parameter vector (representing the instantaneous eigenvalues of each mode), while Equation (3b) defines a drifting trend model for the parameter vector, in which the updated parameter value is equal to the previous value plus some random increment. On the other hand, Equation (3c) is equivalent to Equation (1a).

2.2 Definition of the identification problem

The SS modal model in Equation (3) is comprised by four components, namely the observed signal \mathbf{y}_t , the structure (number of modes) M , the hidden variables corresponding to the state and parameter vectors \mathbf{z}_t and $\boldsymbol{\theta}_t$, and the hyperparameters (SS modal model parameters) $\mathcal{P} := \{\boldsymbol{\Psi}, \boldsymbol{\Sigma}_u, \boldsymbol{\Sigma}_v, \boldsymbol{\Sigma}_\varepsilon\}$. From an identification perspective both the hidden variables and the hyperparameters are unknown variables, while the structure may be a-priori given or different structures could be investigated to determine the best one. Thus, given the signal $\mathbf{y}_1^N := \{\mathbf{y}_1, \mathbf{y}_2, \dots, \mathbf{y}_N\}$ and a structure M , the objective of the identification problem is to determine both the hidden variables $\{\mathbf{z}_1^N, \boldsymbol{\theta}_1^N\}$

and hyperparameters \mathcal{P} that best fit the available data. In turn, this task may be split in two parts:

Estimation of the state and parameter trajectories If hyperparameters were available, then Kalman filtering and fixed interval smoothing can be performed to calculate the distribution of the state and parameter trajectories given data and hyperparameters. The filtering and smoothing procedures aim at calculating the joint posterior distribution of the state and parameter vectors, so that the following probability density functions (PDFs) are calculated (Shumway and Stoffer, 2011, pp. 326-330):

$$p(\mathbf{z}_t, \boldsymbol{\theta}_t | \mathbf{y}_1^t, \mathcal{P}) = \mathcal{N} \left(\begin{bmatrix} \hat{\mathbf{z}}_t^t \\ \hat{\boldsymbol{\theta}}_t^t \end{bmatrix}, \begin{bmatrix} \mathbf{P}_{z_t}^t & \mathbf{P}_{z_t, \theta_t}^t \\ \mathbf{P}_{\theta_t, z_t}^t & \mathbf{P}_{\theta_t}^t \end{bmatrix} \right) \quad (8a)$$

$$p(\mathbf{z}_t, \boldsymbol{\theta}_t | \mathbf{y}_1^N, \mathcal{P}) = \mathcal{N} \left(\begin{bmatrix} \hat{\mathbf{z}}_t^N \\ \hat{\boldsymbol{\theta}}_t^N \end{bmatrix}, \begin{bmatrix} \mathbf{P}_{z_t}^N & \mathbf{P}_{z_t, \theta_t}^N \\ \mathbf{P}_{\theta_t, z_t}^N & \mathbf{P}_{\theta_t}^N \end{bmatrix} \right) \quad (8b)$$

based on the initial conditions:

$$p(\mathbf{z}_0, \boldsymbol{\theta}_0) = \mathcal{N} \left(\begin{bmatrix} \hat{\mathbf{z}}_0 \\ \hat{\boldsymbol{\theta}}_0 \end{bmatrix}, \begin{bmatrix} \boldsymbol{\Sigma}_{z_0} & \\ & \boldsymbol{\Sigma}_{\theta_0} \end{bmatrix} \right)$$

where $\hat{\mathbf{z}}_t^t := \mathbb{E}\{\mathbf{z}_t | \mathbf{y}_1^t, \mathcal{P}\}$ and $\hat{\mathbf{z}}_t^N := \mathbb{E}\{\mathbf{z}_t | \mathbf{y}_1^N, \mathcal{P}\}$ define the expected value of the state vector at time t based on data up to time t (filtering) and up to time N (fixed-interval smoothing), with associated covariances $\mathbf{P}_{z_t}^t := \mathbb{E}\{(\mathbf{z}_t - \hat{\mathbf{z}}_t^t)(\mathbf{z}_t - \hat{\mathbf{z}}_t^t)^\top | \mathbf{y}_1^t, \mathcal{P}\}$ and $\mathbf{P}_{z_t}^N := \mathbb{E}\{(\mathbf{z}_t - \hat{\mathbf{z}}_t^N)(\mathbf{z}_t - \hat{\mathbf{z}}_t^N)^\top | \mathbf{y}_1^N, \mathcal{P}\}$. Similar definitions apply for the parameter vector and the cross-covariance matrices $\mathbf{P}_{z_t, \theta_t}^t$ and $\mathbf{P}_{z_t, \theta_t}^N$. Due to the bilinearity between the state and parameter vectors in the state transition equation (Eq. (3a)), a proper linearization method is required (extended or sigma-point Kalman filters) (Wan and van der Merwe, 2001). Here, the extended Kalman filter/smoothers is appraised.

Hyperparameter estimation On the other hand, if the state/parameter trajectories were known, estimates of the hyperparameters and initial conditions could be performed based on the log-likelihood:

$$\begin{aligned} -2 \ln \mathcal{L}(\mathcal{P}) &= \ln |\boldsymbol{\Sigma}_{z_0}| + (\mathbf{z}_0 - \hat{\mathbf{z}}_0)^\top \boldsymbol{\Sigma}_{z_0}^{-1} (\mathbf{z}_0 - \hat{\mathbf{z}}_0) \\ &\quad \ln |\boldsymbol{\Sigma}_{\theta_1}| + (\boldsymbol{\theta}_0 - \hat{\boldsymbol{\theta}}_0)^\top \mathbf{P}_{\theta_1}^{-1} (\boldsymbol{\theta}_0 - \hat{\boldsymbol{\theta}}_0) \\ &\quad N \ln |\boldsymbol{\Sigma}_u| + \sum_{t=1}^N \mathbf{u}_t^\top \boldsymbol{\Sigma}_u^{-1} \mathbf{u}_t \\ &\quad N \ln |\boldsymbol{\Sigma}_v| + \sum_{t=1}^N \mathbf{v}_t^\top \boldsymbol{\Sigma}_v^{-1} \mathbf{v}_t \\ &\quad N \ln |\boldsymbol{\Sigma}_\varepsilon| + \sum_{t=1}^N \boldsymbol{\varepsilon}_t^\top \boldsymbol{\Sigma}_\varepsilon^{-1} \boldsymbol{\varepsilon}_t \end{aligned} \quad (9)$$

where, from equation (3), $\mathbf{u}_t = \mathbf{z}_t - \mathbf{M}(\boldsymbol{\theta}_{t-1})\mathbf{z}_{t-1}$, $\mathbf{v}_t = \boldsymbol{\theta}_t - \boldsymbol{\theta}_{t-1}$ and $\boldsymbol{\varepsilon}_t = \mathbf{y}_t - \boldsymbol{\Psi}\mathbf{z}_t$.

Since the state and parameter trajectories are unknown, the likelihood in Equation (9) cannot be optimized directly. Instead, smoothed state/parameter estimates and hyperparameters are iteratively refined with the help of an *Expectation-Maximization* (EM) algorithm (Shumway and Stoffer, 2011, Sec. 6.3). Formally, the hyperparameters on iteration j are obtained from the optimization of the objective function (Shumway and Stoffer, 2011, p. 340):

$$\mathcal{Q}(\mathcal{P} | \mathcal{P}_{j-1}) := \mathbb{E} \{-2 \ln \mathcal{L}(\mathcal{P}) | \mathbf{y}_1^N, \mathcal{P}_{j-1}\} \quad (10)$$

based on the PDF of the smoothed state/parameters conditional on the available data and previous hyperparameter guess \mathcal{P}_{j-1} . Applying the definition in Eq. (10) on the likelihood in Eq. (9) yields:

$$\begin{aligned} \mathcal{Q}(\mathcal{P} | \mathcal{P}_{j-1}) &= \ln |\boldsymbol{\Sigma}_{z_0}| + \ln |\boldsymbol{\Sigma}_{\theta_0}| \\ &\quad + \text{tr} \left\{ \boldsymbol{\Sigma}_{z_0} \left(\mathbf{P}_{z_0}^N + (\hat{\mathbf{z}}_0^N - \hat{\mathbf{z}}_0)(\hat{\mathbf{z}}_0^N - \hat{\mathbf{z}}_0)^\top \right) \right\} \\ &\quad + \text{tr} \left\{ \boldsymbol{\Sigma}_{\theta_0} \left(\mathbf{P}_{\theta_0}^N + (\hat{\boldsymbol{\theta}}_0^N - \hat{\boldsymbol{\theta}}_0)(\hat{\boldsymbol{\theta}}_0^N - \hat{\boldsymbol{\theta}}_0)^\top \right) \right\} \\ &\quad + N \ln |\boldsymbol{\Sigma}_u| + N \ln |\boldsymbol{\Sigma}_v| + N \ln |\boldsymbol{\Sigma}_\varepsilon| \\ &\quad + \text{tr} \left\{ \boldsymbol{\Sigma}_u^{-1} (\mathbf{S}_{z_{11}} - \mathbf{S}_{z_{10}} - \mathbf{S}_{z_{10}}^\top + \mathbf{S}_{z_{00}}) \right\} \\ &\quad + \text{tr} \left\{ \boldsymbol{\Sigma}_v^{-1} (\mathbf{S}_{\theta_{11}} - \mathbf{S}_{\theta_{10}} - \mathbf{S}_{\theta_{10}}^\top + \mathbf{S}_{\theta_{00}}) \right\} \\ &\quad + \text{tr} \left\{ \boldsymbol{\Sigma}_\varepsilon^{-1} \mathbf{S}_y \right\} \end{aligned} \quad (11)$$

where:

$$\begin{aligned} \mathbf{S}_{z_{11}} &:= \sum_{t=2}^N \left(\hat{\mathbf{z}}_t^N (\hat{\mathbf{z}}_t^N)^\top + \mathbf{P}_{z_t}^N \right) \\ \mathbf{S}_{z_{10}} &:= \sum_{t=2}^N \left(\hat{\mathbf{z}}_t^N (\hat{\mathbf{z}}_{t-1}^N)^\top + \mathbf{P}_{z_t, z_{t-1}}^N \right) \mathbf{M}^\top (\hat{\boldsymbol{\theta}}_{t-1}^N) \\ \mathbf{S}_{z_{00}} &:= \sum_{t=1}^{N-1} \mathbf{M}(\hat{\boldsymbol{\theta}}_{t-1}^N) \left(\hat{\mathbf{z}}_t^N (\hat{\mathbf{z}}_t^N)^\top + \mathbf{P}_{z_t}^N \right) \mathbf{M}^\top (\hat{\boldsymbol{\theta}}_{t-1}^N) \\ \mathbf{S}_{\theta_{11}} &:= \sum_{t=2}^N \left(\hat{\boldsymbol{\theta}}_t^N (\hat{\boldsymbol{\theta}}_t^N)^\top + \mathbf{P}_{\theta_t}^N \right) \\ \mathbf{S}_{\theta_{10}} &:= \sum_{t=2}^N \left(\hat{\boldsymbol{\theta}}_t^N (\hat{\boldsymbol{\theta}}_{t-1}^N)^\top + \mathbf{P}_{\theta_t, \theta_{t-1}}^N \right) \\ \mathbf{S}_{\theta_{00}} &:= \sum_{t=1}^{N-1} \left(\hat{\boldsymbol{\theta}}_t^N (\hat{\boldsymbol{\theta}}_t^N)^\top + \mathbf{P}_{\theta_t}^N \right) \\ \mathbf{S}_y &:= \sum_{t=2}^N \left(\hat{\boldsymbol{\varepsilon}}_t^N (\hat{\boldsymbol{\varepsilon}}_t^N)^\top + \boldsymbol{\Psi} \mathbf{P}_{z_t}^N \boldsymbol{\Psi}^\top \right) \end{aligned}$$

and where $\hat{\boldsymbol{\varepsilon}}_t^N := \mathbf{y}_t - \boldsymbol{\Psi}\hat{\mathbf{z}}_t^N$ is the smoothing error, and $\mathbf{P}_{z_t, z_{t-1}}^N$ and $\mathbf{P}_{\theta_t, \theta_{t-1}}^N$ are the lag-one state and parameter covariances, calculated with the smoother defined by Property 6.3 in (Shumway and Stoffer, 2011, p. 334), and $\text{tr} \{\cdot\}$ indicates the trace operator of the matrix in the argument.

The conditional expectation of the log-likelihood in Eq. (11) can then be differentiated and equated to zero to find the hyperparameter values and initial conditions yielding a minimum. Following this procedure, and after proper algebraic manipulations, the following update equations are obtained:

Hyperparameter update:

$$\boldsymbol{\Psi}_j = \left(\sum_{t=2}^N \mathbf{y}_t (\hat{\mathbf{z}}_t^N)^\top \right) \mathbf{S}_{z_{11}}^{-1} \quad (12a)$$

$$\boldsymbol{\Sigma}_{\varepsilon_j} = (N-1)^{-1} \mathbf{S}_y \quad (12b)$$

$$\boldsymbol{\Sigma}_{u_j} = (N-1)^{-1} \text{diag}(s_1, s_1, s_2, s_2, \dots, s_M, s_M) \quad (12c)$$

$$s_m = [\mathbf{S}_{z_{11}} - \mathbf{S}_{z_{10}} - \mathbf{S}_{z_{10}}^\top + \mathbf{S}_{z_{00}}]_{2m, 2m} \quad (12d)$$

$$\boldsymbol{\Sigma}_{v_j} = (N-1)^{-1} (\mathbf{S}_{\theta_{11}} - \mathbf{S}_{\theta_{10}} - \mathbf{S}_{\theta_{10}}^\top + \mathbf{S}_{\theta_{00}}) \quad (12e)$$

Initial condition update:

$$\hat{\mathbf{z}}_0 = \hat{\mathbf{z}}_0^N \quad \Sigma_{z_0} = \mathbf{P}_{z_0}^N \quad (12f)$$

$$\hat{\boldsymbol{\theta}}_0 = \hat{\boldsymbol{\theta}}_0^N \quad \Sigma_{\theta_0} = \mathbf{P}_{\theta}^N \quad (12g)$$

where $\text{diag}(\cdot)$ indicates the a diagonal matrix with the elements indicated in the argument, and $[\mathbf{C}]_{k,j}$ indicates the $\{k,j\}$ -th element of matrix \mathbf{C} . Note that only the elements of the diagonal of the state innovations matrix are calculated, instead of the full matrix. This selection is made to preserve the diagonal structure of this matrix, and thus ensure the orthogonality of the modal components.

Summary of the identification algorithm The identification algorithm via EM can be summarized in the following two steps: (i) calculation of the expected conditional log-likelihood in Equation (11) by means of the Kalman filter/smoothing recursions (expectation step), (ii) hyperparameter updating by maximization of the expected conditional log-likelihood via Equation (12) (maximization step). Both steps are iterated until a prescribed number of iterations is achieved or until some convergence criteria is met. The algorithm needs to be initialized with a first guess of the hyperparameters and initial conditions. Due to the complexity of the identification problem, aggravated by the underlying non-linearity of the SS modal model, it is essential to provide good starting values to improve the chances of convergence to the best possible solution. To this end, traditional stationary modal analysis can be used on a short segment of the signal, and then the obtained results can be used as initial values for non-stationary modal analysis.

3. NUMERICAL EXAMPLE

3.1 Signal definition

A multivariate signal of dimensionality $n = 2$, defined as the superposition of three non-stationary sinusoids is considered. The modal components are defined as in the numerical analysis presented in (Avendaño et al., 2018), where the IA and IF of each mode obey the following laws:

$$\begin{aligned} A_{1,t} &= A_{1,0} + A_{1,1} \cos 2\pi T_s \alpha_1 t \\ A_{2,t} &= A_{2,0} + A_{2,1} \sin 2\pi T_s \alpha_2 t \\ A_{3,t} &= \max(A_{3,0} + A_{3,1} |\cos 2\pi T_s \alpha_3 t|, 0) \\ f_{1,t} &= f_{1,0} + f_{1,1} \sin 2\pi T_s \alpha_1 t \\ f_{2,t} &= f_{2,0} + f_{2,1} \sin 2\pi T_s \alpha_1 t \\ f_{3,t} &= f_{3,0} + f_{3,1} \sin 2\pi T_s \alpha_3 t \end{aligned}$$

The multivariate signal is then constructed by the superposition of individual modes, according to:

$$\mathbf{y}_t = \sum_{m=1}^3 \boldsymbol{\psi}_m x_{m,t} + \boldsymbol{\varepsilon}_t \quad (13a)$$

$$x_{m,t} = A_{m,t} \cdot e^{j\phi_{m,t}}, \quad \phi_{m,t} = \phi_{m,0} + 2\pi \sum_{\tau=1}^t f_{m,\tau} \quad (13b)$$

where $\phi_{m,0}$ is the initial phase, which is a uniformly distributed random variable in the range $[-\pi, \pi)$, $\boldsymbol{\psi}_m$ is the m -th mixing vector, with $m = 1, 2, 3$, and $\boldsymbol{\varepsilon}_t$ is a zero-mean NID noise with covariance $\Sigma_{\varepsilon} = \sigma_{\varepsilon}^2 \mathbf{I}$, with σ_{ε}^2 adjusted so that a SNR of 10 dB is obtained. The IA and IF coefficients, the mixing matrix and other signal properties are summarized in Table 1.

Table 1. Signal properties – Example 1

IA and IF coefficients					
m	$A_{m,0}$	$A_{m,1}$	$f_{m,0}$	$f_{m,1}$	α_m
1	1.0	0.2	50	-20	0.50
2	0.8	0.4	80	20	0.50
3	-0.2	1.0	120	20	0.25
Mixing vectors					
$\boldsymbol{\psi}_1 = \begin{bmatrix} 1.0 - j0.8 \\ 0.5 - j0.5 \end{bmatrix}, \boldsymbol{\psi}_2 = \begin{bmatrix} 0.5 - j0.5 \\ 0.8 - j0.1 \end{bmatrix}, \boldsymbol{\psi}_3 = \begin{bmatrix} 0.2 - j0.8 \\ 0.4 - j0.6 \end{bmatrix}$					
Sampling and noise properties					
$N = 3000$ samples, $T_s = 1/500$ s, $SNR = 10$ dB					

Based on the definitions of Eq. (13) and Table 1, a signal of $N = 3000$ samples, with a sampling period $T_s = 1/500$ s is generated. A typical realization of the signal is shown in Figure 1 while the respective IF and IA trajectories are shown in Figs. 2 and 3. The modal decomposition of this signal is challenging since it features two types of singularities: (i) modes 1 and 2 have periodic frequency crossings at times $t = 1.25 + T_1$ s and $t = 1.75 + T_1$ s, with $T_1 = 2$ s; (ii) the amplitude of mode 3 periodically vanishes for about 400 ms around times $t = 1 + T_1$ s, with $T_1 = 2$ s. The issues of traditional non-parametric estimators of IA and IF on this type of signal have been demonstrated in (Avendaño et al., 2018).

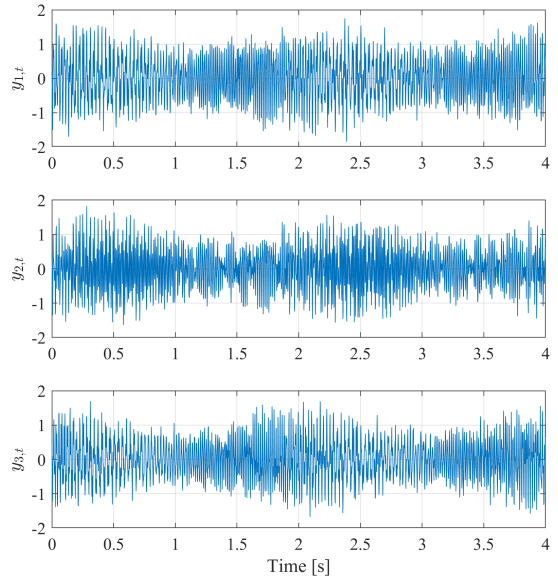


Fig. 1. Typical realization of the signal defined by Eq. (13)

3.2 Estimation of modal components

A multivariate signal generated by the model defined by Equation (13) and Table 1 is used for modal analysis with the TD-SS modal model. The proposed modal estimation method is studied in two modalities:

- (1) *Manual adjustment*: The state and parameter covariances are manually adjusted (by trial and error) to $\Sigma_u = 10^{-4} \mathbf{I}$ and $\Sigma_v = 10^{-5} \mathbf{I}$. The mixing matrix, noise covariance and initial conditions are set by short-time modal analysis based on a 2-nd order Vector AutoRegressive (VAR) model estimated from the first 600 signal samples.

- (2) *EM optimization*: Hyperparameters and initial conditions are optimized with the EM algorithm. The EM algorithm is initialized based on the results of modal analysis from a 2-nd order VAR model calculated from the first 600 signal samples. The state and parameter innovations covariances are initialized as $\Sigma_u = 10^{-5}\mathbf{I}$ and $\Sigma_v = 10^{-6}\mathbf{I}$. The algorithm runs up to 60 iterations or until the norm of the change in the hyperparameters is less than 10^{-6} .

Figures 2 and 3 display the original IF and IA trajectories along with their respective estimates obtained with manual adjustment and EM hyperparameter optimization. The elements of the diagonal of the noise, state and parameter covariance matrices are shown in Figure 4, while a depiction of the full parameter innovations correlation structure is displayed in Figure 5.

The IF and IA estimates shown in Figures 2 and 3 demonstrate a clear improvement after the EM optimization. In the IF estimates, the improvement is mainly evidenced in the reduced duration of the initial transient and overall tracking error. Indeed, it appears as the IF tracking error in mode 2 increases after the frequency crossings in the manually adjusted method. Similarly, in the IA estimates, the initial transient and overall error is increased, especially in mode 3, which exhibits vanishing amplitude.

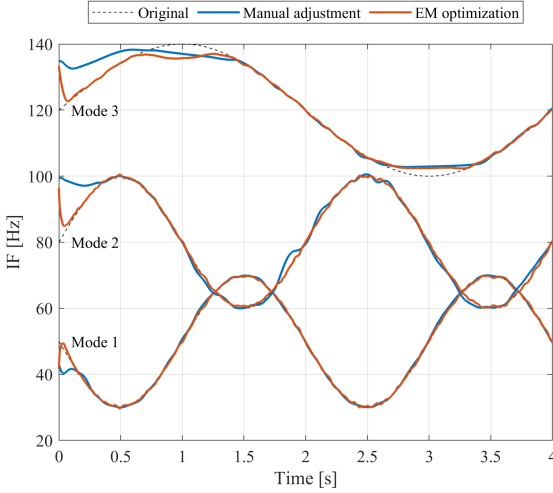


Fig. 2. IF estimates before and after EM optimization compared with the original values.

Figures 4 and 5 evidence the effect of the EM optimization in the state and parameter innovations covariances. Regarding to the state innovations covariance, the algorithm moves from equal variances for all the states to independent values for each pair of states encoding the in-phase and quadrature components of each mode. Similarly, the diagonal elements of the parameter innovations covariance are also modified according to the rate of variation of each mode, but more importantly, as evident in Figure 5, the algorithm evolves from a diagonal to a full structure, which explains very well the correlations between the modal parameters. For instance, the full covariance structure can explain that modes 1 and 2, with parameters indexed 1 to 4, are highly correlated. Indeed, when comparing the IFs in Figure 2, it can be observed that the IFs of modes 1

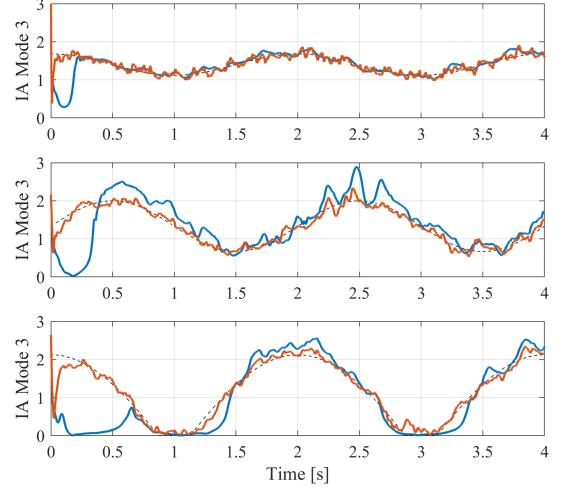


Fig. 3. IA estimates before and after EM optimization compared with the original values.

and 2 evolve with the same sinusoidal pattern, but inverse polarity. As a result, when the EM optimized covariance matrices are used, the Kalman filter/smoothen is not confused by the frequency crossing, since it is informed that these modes should be antisymmetric.

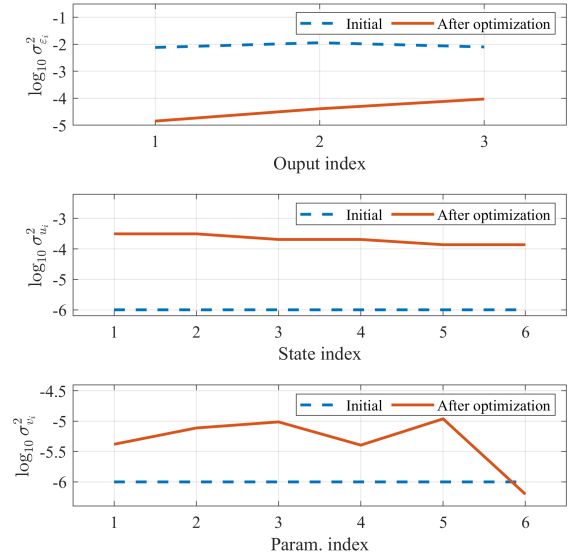


Fig. 4. Diagonal elements of the noise, state and parameter innovations covariances after EM optimization.

Finally, Figure 6 shows the absolute value of the estimates of the mixing vectors for each one of the measured outputs. The cases of the mixing vectors obtained after the VAR-based initialization and after EM optimization are compared with the original values. It can be seen that after EM optimization, the mixing vectors converge quite closely to the actual values.

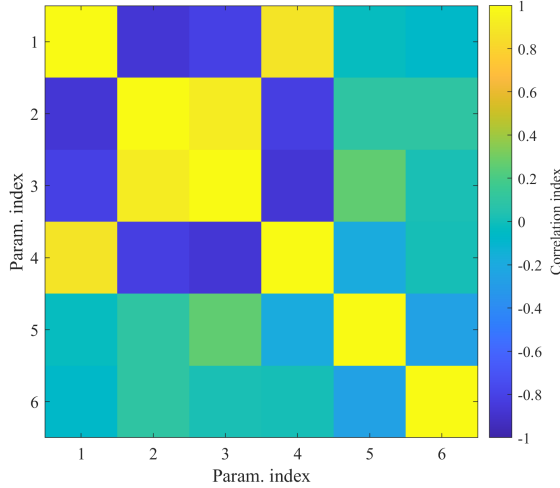


Fig. 5. Correlation index matrix calculated from the parameter innovations covariance after optimization.

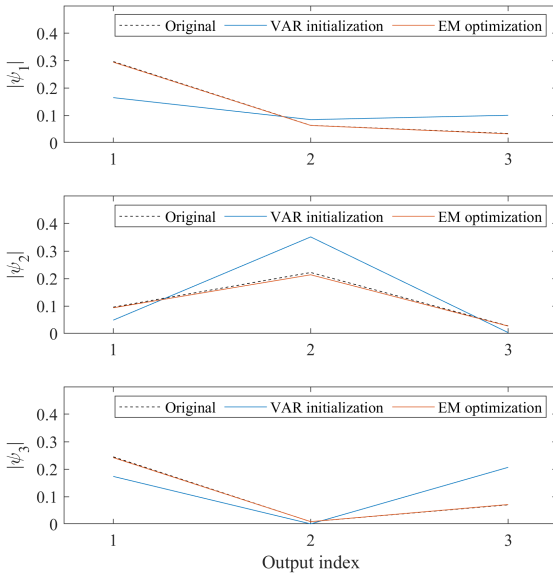


Fig. 6. Modulus of the mixing vector estimates with VAR-based initialization and after EM optimization.

4. CONCLUSION

Direct estimation of modal components of multivariate non-stationary signals via SS modal models has been demonstrated. Proper hyperparameter identification with EM, including full parameter covariance structure, significantly improves the estimation performance of IA and IF even under the presence of singularities.

REFERENCES

Avendaño, L.E., Avendaño-Valencia, L.D., and Delgado-Trejos, E. (2018). Diagonal time dependent state space models for modal decomposition of non-stationary signals. *Signal Processing*, 147, 208–223. doi:10.1016/j.sigpro.2018.01.031.

Boashash, B. (1992). Estimating and interpreting the instantaneous frequency of a signal – part 1: Fundamentals. *Proceedings of the IEEE*, 80(4), 520–538.

Brumana, A. and Piroddi, L. (2020). A multi-tone central divided difference frequency tracker with adaptive process noise covariance tuning. *International Journal of Adaptive Control and Signal Processing*, 34(7), 877–900. doi:10.1002/acs.3111.

Cardona-Morales, O., Avendaño-Valencia, L., and Castellanos-Domínguez, G. (2014). Nonlinear model for condition monitoring of non-stationary vibration signals in ship driveline application. *Mechanical Systems and Signal Processing*, 44(1), 134 – 148. doi:10.1016/j.ymssp.2013.08.029. Special Issue on Instantaneous Angular Speed (IAS) Processing and Angular Applications.

Dardanelli, A., Corbetta, S., Boniolo, I., Savaresi, S., and Bittanti, S. (2010). Model-based Kalman filtering approaches for frequency tracking. *IFAC Proceedings Volumes*, 43(10), 37 – 42. doi:10.3182/20100826-3-TR-4015.00010. 10th IFAC Workshop on the Adaptation and Learning in Control and Signal Processing.

Hao, H., Wang, H., and Rehman, N. (2017). A joint framework for multivariate signal denoising using multivariate empirical mode decomposition. *Signal Processing*, 135, 263 – 273. doi:10.1016/j.sigpro.2017.01.022.

Iatsenko, D., McClintock, P., and Stefanovska, A. (2016). Extraction of instantaneous frequencies from ridges in time-frequency representations of signals. *Signal Processing*, 125, 290 – 303. doi:10.1016/j.sigpro.2016.01.024.

Li, Z., Gao, J., Li, H., Zhang, Z., Liu, N., and Zhu, X. (2020). Synchroextracting transform: The theory analysis and comparisons with the synchrosqueezing transform. *Signal Processing*, 166, 107243. doi:10.1016/j.sigpro.2019.107243.

Lu, K., Jin, Y., Chen, Y., Yang, Y., Hou, L., Zhang, Z., Li, Z., and Fu, C. (2019). Review for order reduction based on proper orthogonal decomposition and outlooks of applications in mechanical systems. *Mechanical Systems and Signal Processing*, 123, 264 – 297. doi:10.1016/j.ymssp.2019.01.018.

Shumway, R.H. and Stoffer, D.S. (2011). *Time series analysis and its applications*. Springer, third edition.

Spiridonakos, M. and Fassois, S. (2009). Parametric identification of a time-varying structure based on vector vibration response measurements. *Mechanical Systems and Signal Processing*, 23(6), 2029 – 2048. doi:10.1016/j.ymssp.2008.11.004. Special Issue: Inverse Problems.

Stanković, L., Brajović, M., Daković, M., and Mandić, D. (2020). On the decomposition of multichannel nonstationary multicomponent signals. *Signal Processing*, 167, 107261. doi:10.1016/j.sigpro.2019.107261.

Wan, E.A. and van der Merwe, R. (2001). *The Unscented Kalman Filter*, chapter 7, 221–280. John Wiley & Sons, Ltd. doi:10.1002/0471221546.ch7.

Zhou, S.D., Ma, Y.C., Liu, L., Kang, J., Ma, Z.S., and Yu, L. (2018). Output-only modal parameter estimator of linear time-varying structural systems based on vector tar model and least squares support vector machine. *Mechanical Systems and Signal Processing*, 98, 722 – 755. doi:10.1016/j.ymssp.2017.05.026.